Rotation in Suspension of a Rod-Shaped Colloid

Liang Hong,[†] Stephen M. Anthony,[‡] and Steve Granick*[,†,‡,§]

Departments of Materials Science and Engineering, Chemistry, and Physics, University of Illinois, Urbana, Illinois 61801

Received April 28, 2006. In Final Form: June 21, 2006

The simple strategy of coating a closely packed colloid monolayer with a nanometer-thick metal film to connect colloidal spheres and then gently sonicating produces a series of colloid metastructures, including rods and planar sheets. These structures can be fluorescently labeled, which can serve as a probe to monitor their dynamics in complex environments. The metal coating modulates fluorescence emission as these structures rotate in suspension. By analyzing the time sequence of fluorescence images using single-particle tracking techniques, here we measure the rotational dynamics of a rodlike tetramer, quantifying rotation along the long axis.

Introduction

Colloidal-sized particles (larger than molecules but small enough to sustain Brownian motion) are fundamental in nature and technology.[1] Their phase behavior is central to a large variety of applications, such as paints, ceramics, and photonic materials.[2] They also serve as models of atoms to study crystal growth,[3,4] glass transitions,[5,6] and material fracture.[7,8] However, spherical shape is only one possibility. To extend the possibilities, ellipsoids, rods, and plates have been synthesized.[9] Alternatively, uniform spherical particles can be formed into colloidal clusters, which are expected to have more unusual symmetry.[7] For example, Manoharan and Pine prepared a series of clusters based on an emulsion technique. Those clusters are rigid but are restricted to structures with high symmetry.[10,11]

In this paper, we describe preparation of a series of colloid clusters with lower symmetry, such as rodlike structures, using metal deposition onto a close-packed colloidal monolayer followed by gentle sonication. Owing to the directionality of the metal beam, only one hemisphere of the particles is coated. This metal layer serves as a welding material to connect particles together. During sonication, the monolayers break up into randomly shaped planar structures including rods. Although this method is not efficient at this stage, there are three distinct advantages. First, these structures have much lower symmetry. Potentially, these rodlike structures can serve as models for a new category of colloidal-sized analogues of molecules, such as liquid crystals or rigid biopolymers. Second, metal coating provides an excellent starting point for various chemical modifications. Going beyond the geometrical factor, we can incorporate surface functionalization into these colloidal analogues of molecules.[12] Third, metal coating modulates the fluorescence emitted from these structures. In a sense, we can view these rodlike structures as a few connected MOONs (modulated optical nanoparticles).[13] This feature not only provides a way to identify orientation but also to measure rotational diffusion along the long axis, which is otherwise difficult to observe. We discuss this measurement in detail below.

Rotational diffusion measurement has been widely employed for more than a century to look at small molecule dynamics and interaction. However, few rotational experiments concern colloidal sized particles.[14,15] The reason is that the well-developed techniques useful for molecules, such as fluorescence anisotropy, cannot scale-up to colloidal sized particles, as the rotational time constant becomes longer than the lifetime of a fluorescent molecule. Moreover, photobleaching is a serious problem in this time window. However, rotational diffusion measurements of spherical colloids with single-particle resolution were recently developed by Kopelmann using the idea that coating one hemisphere with metal blocks excitation as well as fluorescence emission from this hemisphere.[13,16]

Here we rationally extend this idea to new colloidal structures. Based on single-particle tracking techniques, we develop an algorithm to measure the rotational dynamics of a rodlike tetramer, in particular quantifying rotation around the long axis for the first time. This technique opens the door toward fully understanding the dynamics of rodlike structures in different environments, and also provides a sensitive probe for microrheological measurements.

Experiment and Data Analysis

Sample Preparation. The colloidal particles used in this study were 1 μm diameter carboxylate-modified polystyrene latex particles labeled with nile-red (Invetrogen Inc.). A 50μL aqueous solution of these particles (2% solid) was spread uniformly onto a glass slide treated with piranha solution. The colloidal particles formed a close-packed monolayer during the evaporation of the solvent. This substrate was then coated with 2 nm of titanium followed by 50 nm

* To whom correspondence should be addressed.
[†] Department of Materials Science and Engineering.
[‡] Department of Chemistry.
[§] Department of Physics.

(1) Israelachvili, J. N. *Intermolecular and Surface Forces*, 2nd ed.; Academic: San Diego, CA, 1992.
(2) Qi, M. H.; Lidorikis, E.; Rakich P. T.; Johnson S. G.; Joannopoulos, J. D.; Ippen, E. P.; Smith, H. I. *Nature* **2004**, *429*, 538.
(3) Pusey, P. N.; Van Megen, W.; Barlett, P.; Ackerson, B. J.; Rarity, J. G.; Underwood, S. M. *Phys. Rev. Lett.* **1998**, *63*, 2753.
(4) Gasser, U.; Weeks, E. R.; Schofield, A.; Pusey, P. N.; Weitz, D. *Science* **2003**, *292*, 258.
(5) van Blaaderen, A.; Wiltzius, P. *Science* **1995**, *270*, 1177.
(6) Yetrihaj, A.; van Blaaderen, A. *Nature* **2003**, *421*, 513.
(7) van Blaaderen, A. *Science* **2003**, *301*, 470.
(8) Schall, P.; Cohen, I.; Weitz, D.; Spaepen, F. *Science* **2004**, *305*, 1948.
(9) Sacanna S.; Rossi L.; Kuipers B. W. M.; Philipse A. P. *Langmuir* **2006**, *22*, 822.
(10) Manoharan, V. N.; Elsesser, M. T.; Pine, D. J. *Science* **2003**, *301*, 483.
(11) Yi, G.-R.; Manoharan, V. N.; Michel, E.; Elsesser, M. T.; Yang, S.-M.; Pine, D. J. *Adv. Mater.* **2004**, *16*, 1204.
(12) Hong, L.; Cacciuto, A.; Luijten, E.; Granick, S., submitted.
(13) Behrend, C. J.; Anker, J. N.; Kopelman, R. *Appl. Phys. Lett.* **2004**, *84*, 154.
(14) Andablo-Reyes, E.; Diaz-Leyva, P.; Arauz-Lara, J. L. *Phys. Rev. Lett.* **2005**, *94*, 106001.
(15) Barrall, G. A.; Schmidt-Rohr, K.; Lee, Y. K.; Landfester, K.; Zimmermann, H.; Chingas, G. C.; Pines, A. *J. Chem. Phys.* **1996**, *104*, 509.
(16) Behrend, C. J.; Anker, J. N.; McNaughton, B. H.; Brasuel, M.; Philbert, M. A.; Kopelman, R. *J. Phys. Chem.* **2004**, *108*, 10408.

10.1021/la061169e CCC: $33.50
Published on Web 07/12/2006

of gold in an AJA sputtering machine. The resulting substrate was sonicated gently in water for 5 min in order to detach the colloidal particles from the surface.

Sample Characterization. Epifluorescence microscopy was used to image the colloidal structures. We employed a 532 nm laser and focused it at the back focal point of a 63× objective. The fluorescence image was collected using this same objective, and the time sequences of images ("movies") were recorded by an electron multiplying CCD camera (Andor Ixon) after filtering out light from the excitation laser. The time-dependent data analyzed below was recorded with an exposure time of 0.1 s for 800 frames. The concentration of the particles was less than 0.1% in a 4:1 water and glycerol solution. These conditions ensured no multi-body interactions and that the rotation was slow enough to measure easily. We also made certain that the rodlike structures remained in focus throughout the measurement.

Further characterization was made using scanning electron microscopy (SEM). The polystyrene beads were dissolved by chloroform and the gold coating structure was imaged using an SEM microscope (JEOL. 6060LV).

Image Analysis. To determine the time-dependent angle when a particle rotates, first the particle must be located. Image analysis was accomplished using modified implementations of standard particle tracking algorithms.[17,18]

Quantification of the angle along the long axis was based on the "moon" effect introduced by Kopelmann and co-workers.[16] Assuming that a sphere possesses one uniformly bright hemisphere and one dark (invisible) hemisphere, the total brightness of the feature can be expressed as

$$A(1 + \cos\theta) \tag{1}$$

where $\theta = 0$ corresponds to the bright hemisphere pointing directly at the observer and $\theta = 180°$ corresponds to the dark hemisphere pointing directly at the observer. In practice, the features never reach zero brightness, both because of the background intensity and because the hemispheres are imperfect. However, over long enough time sequences, eventually all orientations of the moon are observed. Therefore, the range of brightness can be rescaled, setting the dimmest measured value to be the background and the brightest measured value to be 2*A*. In the case of slightly nonhemispherical coating, this introduces a systematic error which will increase the measured angle changes by approximately

$$\Delta\theta_{\text{observed}} \cong \Delta\theta_{\text{real}} \frac{90}{X} \tag{2}$$

where X is the number of degrees coated when measured from the zenith. In cases where the degree of coating is known, this error can be largely corrected.

This experiment concerned linear tetramer rods comprised of colloidal spheres. The magnification used was sufficient to distinguish the four component MOONs of the rod, allowing determination of the overall orientation of the rod. Visual analysis of the rotation showed that rotation of the long axis of the rod was slow on the time scale of the data acquisition. Thus, although the rod was free to rotate in any fashion, for analysis, it was possible to select a time sequence where the long axis of the rod remained in the image plane throughout, affording the best chance to observe rotation around the long axis. The brightest local maxima of each image were then considered as candidates for the positions of the four MOONs which made up the rod. Using these maxima as the location of the particle can cause a lateral shift relative to the center of the particle, dependent upon the orientation of the rod. However, although this shift could be corrected, for this analysis, it was ignored, as it only affected the short-time translational dynamics. Although these maxima were invariably along the line of the rod, occasionally the position of one of the MOONs would not register as a maximum, or additional points along the rod would register. However, due to the rigid structure

(17) Crocker, J. C.; Grier, D. G. *J. Colloid Interface Sci.* **1996**, *179*, 298.
(18) Anthony, S.; Zhang, L. F.; Granick, S. *Langmuir* **2006**, *22*, 5266.

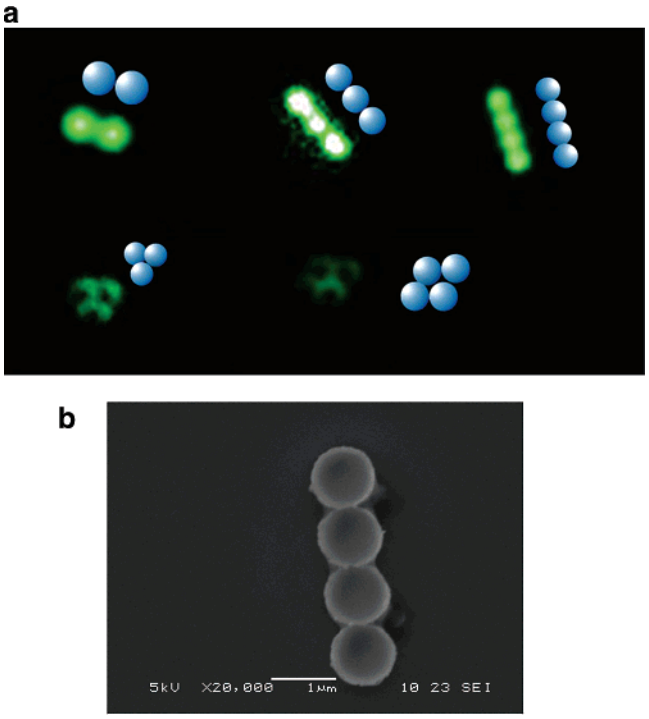

Figure 1. Examples of colloidal metastructures formed after sonicating a close-packed colloidal monolayer coated with gold, the colloids containing fluorescent dye. (a) Images of a linear dimer, trimer, tetramer (top portion of this panel) and also of a triangle and a rhomboid (bottom panel). Dark parts on the planar clusters are due to modulation from the metal coating. In this panel, fluorescence images are accompanied by computer-generated schematic diagrams. (b) SEM (scanning electron micrograph) image of the gold shell of a linear tetramer after dissolving away the colloidal latex particles.

of the rod, geometrical considerations could be used to remove extraneous points and to interpolate or extrapolate missing points. Having localized the MOONs in each frame, positions of the rod in consecutive frames were compared.

As the motion of each of the MOONs forming the rod over the interval between frames was small compared to the size of the rod, the assignment of the trajectory was trivially obvious. The orientation of the rod in the focal plane was easily determined by finding the line that fell through the previously determined positions of the four particles. This portion of the analysis was used for the specific movie analyzed, and the accuracy of the tracking for this time sequence was visually confirmed. After locating the position of the four MOONs, the angle of each of the particles was calculated independently. Comparison of the angles determined for the four particles showed strong correlation, as expected due to the rigid nature of the rod.

The rate of rotation was calculated by constructing a histogram of the displacement over a set number of time frames. For rotation around the long axis of the tetramer, the displacements were calculated for each of the four particles and combined. Based upon the width of the Gaussian function that described the distribution, the diffusion rate was calculated, after compensation for the angular uncertainty. In this case, the bounds upon the zenith angle minimally perturbed the measurement since the typical step only involved a few degrees of rotation.

Results and Discussion

Colloidal Clusters. Figure 1A shows examples of the various metastructures observed when colloidal monolayers coated with gold were broken up by sonication in the manner described above. We observed rodlike structures such as dimers, trimers, and

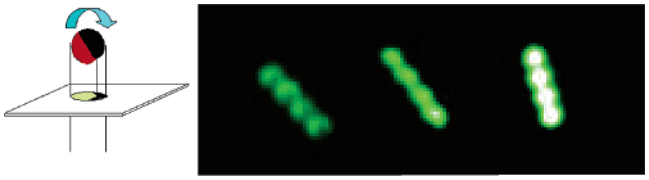

Figure 2. Left panel: schematic diagram of the mechanism of fluorescence modulation of MOON particles. The main point is that one hemisphere is dark because a metal coats it; as a result, particle rotation is observed as fluorescence intensity fluctuation as the particle rotates by Brownian motion, the dark side and the bright side alternatively pointing in the normal direction toward a microscope objective. Right panel: representative fluorescence images for diffusion of a linear tetramer. The different fluorescent intensities in these images correspond to different angles with respect to the normal direction.

tetramers, as well as planar structures such as triangles. These structures were stable and rigid during the whole process, indicating that the stability of these structures is much higher than the thermal energy. Figure 1 shows a linear dimer, trimer, and tetramer and also a triangle and a rhomboid. In the future, greater control of the shape of these clusters may be obtainable through template-assisted self-assembly,[19,20] combined with centrifugal separation of the resultant structures.[21]

These structures were welded together by the metal films that coated them. To show this, we dissolved the polystyrene particles with chloroform. Gold shells remained and were imaged using SEM (Figure 1B). Two important features should be emphasized in this SEM image. First, the diameter of the gold shell is close to that of the original polystyrene particle, so it is reasonable to assume that the metal coating covered just one hemisphere of the particle. This feature makes the rotational diffusion analysis easier, which we will discuss later. Second, even after dissolving the particles, the gold shells between particles remained connected; careful examination of the SEM images shows that a thin film of gold welds the shells together. Control experiments (data not shown here) showed that in order to accomplish this end, the metal film cannot be too thin. To produce the metastructures in Figure 1A, a short sonication time was needed. When the sonication time was longer, this same procedure resulted in mostly homogeneous isolated particles, consistent with known literature in this field.[13,16]

In this study, we selected the metal coating to be gold, in part because its high reflectivity is advantageous for measurement of rotational diffusion and also because of the potential to easily modify the gold surface using well-established thiol chemistry. In this way, numerous different surface chemistries can be generated from these structures.[12] However, besides gold, other metals or metal oxides can also be employed, allowing extension to magnetic and other functional materials.[22]

Rotational Diffusion and Analysis. In Figure 2, a series of snapshots from a movie of a rodlike tetramer in which the fluorescence emission was modulated by the metal coating, shows the mechanism to observe the moon effect by analysis of a time series of fluorescence data. Throughout the experimental time frame, the dark sides of the rod remain connected. This confirms the rigidity of the structure and that within the cluster there is no internal relative rotation. The main point is that these structures rotated rigidly in suspension by Brownian motion.

Data such as that illustrated in Figure 2 shows the coexistence of in-plane rotational diffusion and rotation along the long axis. In other movies, out-of-plane rotation was also observed. However, in this particular movie, it was negligible because the rod cluster sedimented close to the bottom surface of our sample cell due to a density mismatch, and out-of-plane rotation was hindered by the presence of the nearby solid surface. This condition also ensured that the whole structure remained in focus throughout the experimental time window.

We first quantified rotational diffusion along the long axis. Figure 3A shows individual angle trajectories for two of the four particles in the tetramer rod. These trajectories overlap very well; the standard deviation is $<5°$, proving that the rod structure is rigid and our analysis has the needed angular resolution.

Figure 3B shows that the angular displacement histogram is fitted well with a Gaussian profile

$$P(d) = Ae^{-d^2/4Drt} \tag{3}$$

Here, d is the angular displacement at a certain time t, A is a pre-factor, P is the probability of particles rotating, and D_r is the rotational diffusion constant. The good fit is characteristic of Brownian behavior. The diffusion constant for this mode of rotation (D_L) is 140 ± 10 deg^2/s. The misfit at large angular displacements was due to the heterogeneous systematic error in identifying the zenith angle. Particularly when θ is close to 0 or 180, the same intensity change (ΔA) will cause a larger angular change ($\Delta\theta$). To our best knowledge, this is the first quantification of the rotational diffusion of a micron-sized rod around the long axis.

The other degree of freedom, in-plane rotation, was also measured; Figure 3C shows the angular trajectory of this motion. From the Gaussian fit, the diffusion constant (D_I) is 42 ± 5 deg^2/s.

For a comparison to theory of the rotational diffusion of a rod in dilute solution, based on Tirado and Garcia de la Torre's prediction, a cylinder with a length-to-diameter aspect ratio of 4 should give a ratio of rotational diffusion constant $D_L/D_I \approx 5$.[23] However, our rodlike cluster is not a smooth cylinder; instead, it is a series of connected beads. The end effect and the corrugation between beads can change the hydrodynamics substantially. Therefore, a bead model will represent our cluster more faithfully. Here the freely available computer software Hydro, which is based on the bead model, was used to calculate the rotational relaxation times.[24] According to this model, a rod with 4 rigid connected beads shows a ratio of diffusion constants, $D_L/D_I \approx 3.6$, whereas our data shows a ratio of approximately 3.3. This discrepancy may come from the anisotropy of the tetramer from top to bottom owing to the metal coating. Considering the thickness of the metal coating, approximately 10% of the radius, and the resulting density mismatch, our measurements agree reasonably well with the theory.

Differing from previous literature,[16] in this measurement only a short time window is sufficient to quantify the rotational diffusion constant. Better time resolution has been achieved. It is worth emphasizing that while traditional polarization-based measurement of small-molecule rotational diffusion is model-dependent and involves difficulty in resolving the two rotational degrees of freedom, our measurement easily resolves them independently in real space, particle-by-particle.[25] In the future,

(19) Lee, I.; Zheng, H.; Rubner, M. F.; Hammond, P. T. *Adv. Mater.* **2002**, *14*, 572.
(20) Xia, Y.; Yin, Y.; Lu, Y.; McLellan, J. *Adv. Funct. Mater.* **2003**, *13*, 907.
(21) Manoharan, V. N.; Elsesser, M. T.; Pine, D. J. *Science* **2003**, *301*, 483.
(22) Roberts, T. G.; Anker, J. N.; Kopelman, R. *J. Magn. Magn. Mater.* **2005**, *293*, 715.
(23) Eimer, W.; Williamson, J. R.; Boxer, S. G.; Pecora, R. *Biochemistry* **1990**, *29*, 799.
(24) Garcia de la Torre, J.; Navarro, S.; Lopez Martinez, M. C.; Diaz, F. G.; Lope Cascales, J. J. *Biophys. J.* **1994**, *67*, 530.

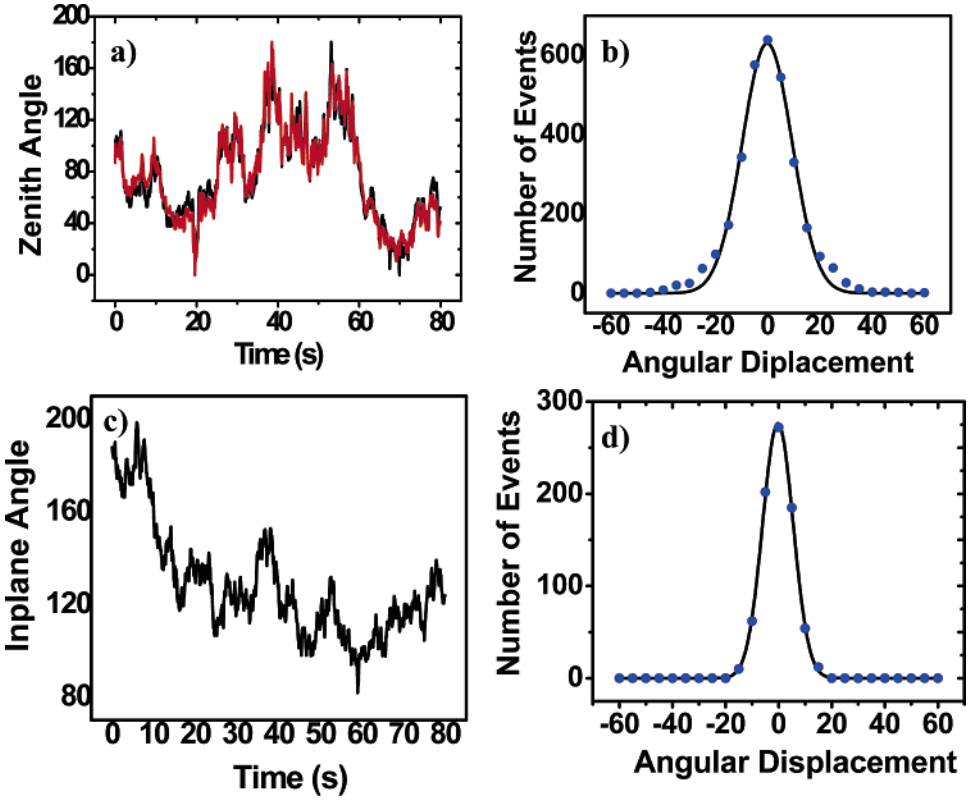

Figure 3. Illustrations of raw data and of its statistical analysis, when single-particle tracking is used to analyze rotation of MOON particles. (a) Zenith angle trajectories of two particles in the linear tetramer. (b) Angular displacement histogram for rotational diffusion along the long axis; angular resolution is approximately 5°. The solid line shows the Gaussian fit, from which we deduce the diffusion constant for this mode of rotation $D_L = 140 \pm 10$ deg^2/s. The misfit at large angular displacements reflects heterogeneous systematic error in identifying the zenith angle. (c) In-plane angle displacement trajectory of this same linear tetramer. (d) Angular displacement histogram for in-plane rotation; angular resolution is approximately 2°. The solid line shows the Gaussian fit, from which we deduce $D_I = 42 \pm 5$ deg^2/s.

this approach will provide a useful model on the basis of which to study the dynamics of connected beads or stiff biopolymers in more complex environments than the dilute solution considered here.

Acknowledgment. L.H. thanks Mr. Hong Zhao for helpful discussion. This work was supported by the Department of Energy under Award No. DEFG02-02ER46019. S.A. acknowledges the NSF for financial support in the form of a Graduate Research Fellowship.

LA061169E

(25) Christensen, R. L.; Drake, R. C.; Phillips, D. *J. Phys. Chem.* **1986**, *90*, 5960.